



Research Article

# Evaluation for Optimal Configuration of Twisted Fiber Bundle Wick Heat Pipe with Top Heat Mode

J. Simsiriwong  
R. Wanison  
P. Sakulchangsatjatai  
P. Terdtoon  
N. Kammuang-lue\*

Department of Mechanical  
Engineering, Faculty of Engineering,  
Chiang Mai University, Chiang Mai,  
50200, Thailand

Received 15 September 2023

Revised 13 November 2023

Accepted 22 November 2023

## Abstract:

*The objective of this research was investigating the thermal resistance of the twisted fiber bundle wick (TFBW) heat pipe. TFBW was made by combining between both size copper fiber of 30  $\mu\text{m}$  and 50  $\mu\text{m}$ . These were arranged as the lengthwise and twist together. The variable parameters of the TFBW were focused on the mixing ratio and twisting pitch length. TFBW heat pipe with outer diameter of 3 mm and length of 70 mm was heated in the top heat mode. Heat input was maintained as constant value at the evaporator section. The condenser section was cooled by air. The outer surface of both sections was measured temperature which were using for calculating the thermal resistance. It was observed that the mixing ratio of 50%:50% demonstrated the lowest thermal resistance for twist pitches of 10 mm and 15 mm. Due to the appropriate pore size of the formed wick, it provided high capillary pressure and high permeability. The decreasing of twist pitch (tighter twisting) caused to increasing of thermal resistance. This was because an excessive twist resulted in very small pore sizes led to lower permeability. The mixing ratio of 50%:50% with a pitch length of 20 mm exhibited an opposite trend because that already had the appropriate pore size. Moreover, the twisting with a smaller pitch had smaller pores leading to a higher capillary pressure. Therefore, the optimal configuration of TFBW providing the lowest thermal resistance was the mixing ratio of 50%:50% with a pitch length of 10 mm.*

**Keywords:** Twisted fiber bundle wick, Pitch length, Mixing ratio, Thermal resistance, Heat pipe

## 1. Introduction

The heat pipe is a specialized device that efficiently transfers heat from the hot area to the cooler ones by using the latent heat of working fluid evaporation. This process happens inside the heat pipe and helps it transfer heat with very low resistance. This quality makes heat pipes excellent at exchanging heat, especially in technical applications like cooling the component of electronic devices, such as computer central processing units (CPUs) and graphics processing units (GPUs), in computer and smartphones.

From Fig. 1, the heat pipe starts working when it absorbs heat from the heat source in direct contact with its evaporator section. Subsequently, the working fluid within the heat pipe transitions into a vapor state, flows through the vapor core towards the condenser section which is contact with a cooling element. Then, the working fluid condense into a

\* Corresponding author: N. Kammuang-lue  
E-mail address: niti@eng.cmu.ac.th



liquid phase and return to the evaporator section by capillary action of the porous media in the heat pipe. Porous materials exhibit a multitude of extremely small pores of varying sizes distributed within them. Each of these pore interconnects and forming numerous capillary tubes, thus causing the phenomenon of capillary action. This is caused by the adhesive force between the water and porous is stronger than the cohesive force between the water molecules. Consequently, porous media can attract liquids, allowing them to flow through. This includes the ability to carry liquids to higher altitudes due to the capillary effect. Therefore, the heat pipe with porous media can be operate in any orientations. Despite the condenser section being higher than the evaporator section, liquid can still flow through the porous media from the evaporator to the condenser. The ability of a porous media depends on the size of the pore, tortuosity and continuity of the pores. That can be divided into 2 parameters which are capillary pressure ( $P_c$ ) and permeability ( $K$ ). Therefore, the capillary pressure ( $P_c$ ) and permeability ( $K$ ) affect the circulation of working fluid inside the heat pipe [1-3].

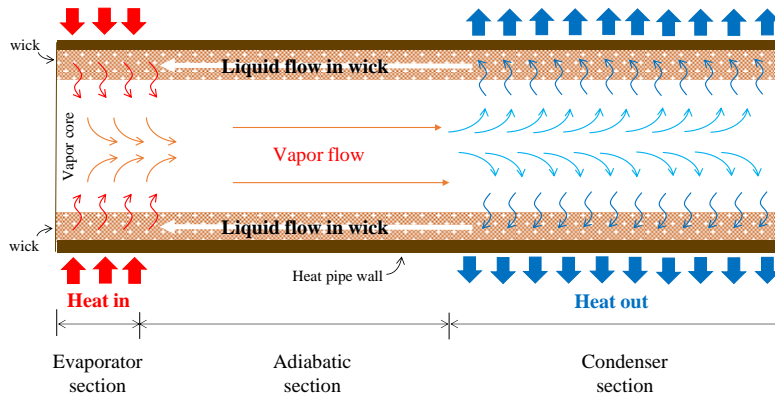


**Fig. 1.** The operation of heat pipe.

The capillary pressure depends on the porosity of porous media which is a proportion of the volume of void space in porous media and the total volume of porous media. The permeability is a parameter indicating the flow resistance that depends on the pore size and pore alignment. The porous media that commonly use in heat pipe, such as axial groove, screen mesh, fiber bundle and sintered powder [4-6] are exhibit difference structural attributes and pore characteristics. Therefore, there are difference of capillary pressure and permeability as show in Fig. 2.

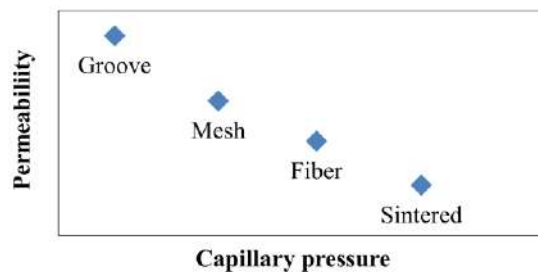


**Fig. 2.** The relationship between capillary pressure and permeability of porous media [6].

As previously, the capillary pressure and the permeability are main variable inducing the thermal performance of heat pipe. In previous work found that the fiber bundle wick provided a high permeability and high capillary pressure. Moreover, it provided a larger vapor core than the metal sintered powder. Especially, the flattening and bending the heat pipe did not damage the fiber bundle wick. Therefore, the fiber bundle wick use as porous media for miniature heat pipes that use to cool the smartphone. Typically, the fiber bundle wick comprises an arrangement of copper fibers with a diameter of 50  $\mu\text{m}$  extending along the length of the wick and twisted to maintain the pore shape and the shape of the bundle [4, 6-8] as shown in Fig. 3. [9]. Twisting with a long pitch causes to the individual fibers to be closer together than twisting with a short pitch. The fiber bundle wick is sintered to attach with only one side of the inner pipe wall. The heat pipe is arranged the fiber bundle side contacting to heat source. As per mention, the heat

pipe receives heat from the heat source by half-pipe at evaporator section. On the other hand, the heat can be release from the condenser section around the pipe as shown in Fig. 4.

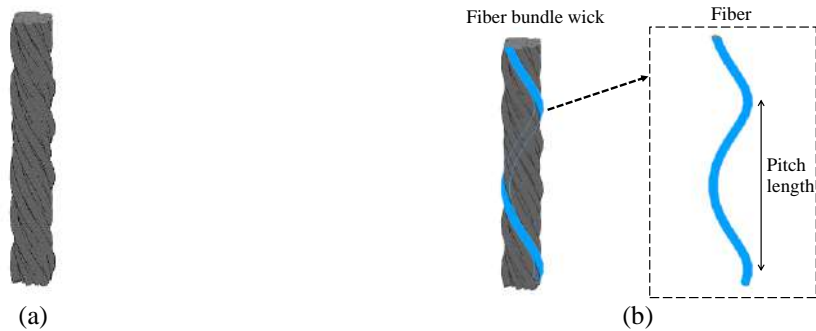


**Fig. 3.** The fiber bundle (a) and the pitch length of fiber bundle (b) [9].

Nowadays, the technology is advancing rapidly, the electronic devices become more compact and higher efficiently which are harder to manage the heat that is generated by their operation. So, the heat pipes need to be efficient within a compact size causing the fibers with a diameter of  $30\mu\text{m}$  are used to produce porous materials. The advantage is a lower porosity as provide higher capillary pressure but it is lower permeability, very expensive and difficult manufacturing process.

In addition, the heat pipe which is used to cool the smartphone working in the top heat mode condition has lower performance then horizontal mode or bottom heat mode. Because the evaporator section is higher than the condenser section. Then, the return working fluid flows against gravity as shown in Fig. 4. Therefore, the porous media requires a higher capillary pressure and higher permeability in order to be able to send the liquid to the evaporator section quickly [10, 11].

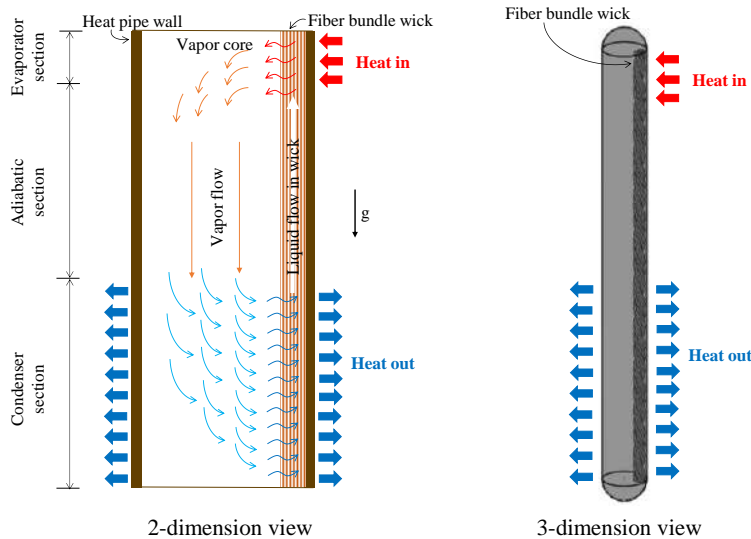


**Fig. 4.** The operation of fiber bundle heat pipe with top heat mode.

Therefore, it is important to develop the fiber bundle wick with higher capillary pressure for operating with the top heat mode heat pipe. Normally, the porous media with low porosity is provided the higher capillary pressure but it has low permeability. However, the fiber bundle wick with low porosity has a high permeability due to the flow channel that is not tortuous like sintered powder.

From previous work, the void simulation model and the void experiment of sintered powder were studied. These were shown that the mixing of various sizes of metal powder induced to the lower porosity than the one size of metal powder. So, it provided a high capillary pressure of sintered powder wick [5, 12-14]. If considering the 2D cross-section that perpendicular to the flow in wick, the characteristics of sintered metal powder wick and the fiber bundle wick were similar. The material areas were circular in shape. Internal void spaces were formed between adjacent circular materials. In the previous research on porous media of the heat pipes, both experimental and simulation studies had been conducted. Most of these studies had focused on sintered powder wick. However, the experimental studies on fiber wick were inadequate study. Moreover, all of these past studies focused on the fiber bundle wick, which was made from only one size of fiber. In manufacturing, it was possible to produce fibers of various sizes, but fiber bundle wick with various sizes of fibers had not yet been produced. Moreover, the orientation of the porous media within only one side of the heat pipe was less studied. This was because the porous media was usually attached to the inside of the heat pipe along the tube's circumference.

Therefore, this research was a study of a new type of porous media for the heat pipes in terms of using mixed fiber sizes and the location of the porous media inside the pipe. So, this research was investigated the thermal performance of the heat pipe, with new configuration of fiber bundle wick these were mixing of 30  $\mu\text{m}$  and 50  $\mu\text{m}$  fibers and twisted with 10, 15 and 20 mm of pitch length for an experimental.

## 2. Materials and Method

The detail of the heat pipe, experimental setup and the experimental procedure were described in this section.

### 2.1 Heat Pipe

The fiber bundle wick heat pipe with a diameter of 3 mm and a length of 70 mm was used in the experiment to determine its thermal performance as shown in Fig. 5. It was constructed from a copper pipe with a diameter of 3 mm and a thickness of 1 mm. The working fluid was deionized water in 100% filling ratio (equal to the void volume of the wick). The void volume ( $V_{\text{void}}$ ) of fiber bundle wick was calculate by Eq. (1).

$$V_{\text{void}} = \pi R_w^2 L - \left( \frac{\pi}{4} d_1^2 N_1 + \frac{\pi}{4} d_2^2 N_2 \right) L \quad (1)$$

Where

$N_1$	was	the number of fiber's diameter 30 $\mu\text{m}$ in fiber bundle wick.
$N_2$	was	the number of fiber's diameter 50 $\mu\text{m}$ in fiber bundle wick.
$d_1$	was	30 $\mu\text{m}$ .
$d_2$	was	50 $\mu\text{m}$ .
$L$	was	the length of bundle.
$R_w$	was	the bundle radius as in Fig. 3(b).

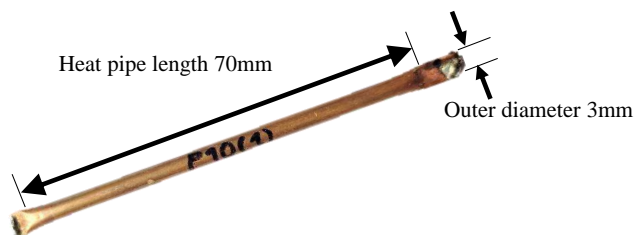


**Fig. 5.** The fiber bundle wick heat pipe.

The fiber bundle wick was composed of copper fibers with diameters of 30 and 50  $\mu\text{m}$ , mixed in different proportions as percentage: 10%:90%, 30%:70%, 50%:50%, 70%:30%, and 90%:10%. The numbers of fibers were presented in Table 1. The number of fibers of each size was determined by setting the bundle boundary with radius of the bundle 0.32 mm for all mixing ratio. Filling both sizes of fibers in reference to the mixing ratio until the bundle was full. The fiber bundle was twisted with pitches of 10, 15, and 20 mm. This was because as per the industrial sector the fiber

bundle wick was produced for using only one size of fiber's diameter. That equaled 50  $\mu\text{m}$  and it was twisted with pitch of 20 mm by using a twisting machine. That machine could be adjusted the pitch to a maximum of 20 mm. Therefore, this research examined the maximum pitch that could be achieved by the industrial sector without additional costs and the lowest pitch studied was 10 mm which was a half of the maximum pitch. Consequently, there consisted for fifteen configurations for the fiber bundle wick.

In the process of heat pipe fabrication, the first step was to prepare a fiber bundle wick with the specified number of fibers of each fiber size as shown in Table 1. After that, these were twisted with a twisting machine according to the desired pitch. Then, the twisted fiber bundle was packed into a copper pipe with diameter of 3 mm and length of 80 mm. As mentioned, it was firmly fixed at both ends of the fiber bundle to prevent deformation. The position of the fiber bundle wick was ensured by arranging it close to one side of the inner pipe wall and sealing one end of the pipe. The connection between the end of the fiber bundle and the other end of the pipe were established by soldering fibers outside the pipe end. Subsequently, the water was added by vacuuming air out of the pipe. After that, the specified amount of water was added to the pipe. Finally, the other end of the pipe were immediately closed.

**Table 1:** Number of fiber's diameter 30  $\mu\text{m}$  and 50  $\mu\text{m}$  of each mixing ratio

Mixing ratio %N <sub>1</sub> : %N <sub>2</sub> (30 $\mu\text{m}$ : 50 $\mu\text{m}$ )	Numbers of fibers	
	Fiber's diameter 30 $\mu\text{m}$ (N <sub>1</sub> )	Fiber's diameter 50 $\mu\text{m}$ (N <sub>2</sub> )
10:90	13	111
30:70	44	101
50:50	85	84
70:30	145	62
90:10	235	26

Where %N<sub>1</sub> was the percentage of fiber's diameter 30  $\mu\text{m}$  in fiber bundle wick.  
 %N<sub>2</sub> was the percentage of fiber's diameter 50  $\mu\text{m}$  in fiber bundle wick.

## 2.2 Experimental Setup

The test rig was shown in Figs. 6 and 7. The heater block comprised a copper block 10x10x2.5 mm and a ceramic heater 40 V, 45 W inside. The DC power supply brand Good Will model GPR-7550D for heater offered adjustable voltage (0-70 V) and current (0-5 A), boasting high precision with a minimal deviation of 0.1%. The heat sink consisted of a 12 V DC electric fan (60 mm in diameter) brand NMB model 2406KL and a tunnel with cross-sectional dimensions of 90x60 mm and a length of 500 mm, incorporating the fan. The DC power supply brand GW Instek GPS-3030D for the fan enabled voltage adjustment within the range of 0-30 V and current adjustment within 0-3 A, maintaining precision with a discrepancy of 0.1%.

The heat pipe was tested in vertical orientation which the evaporator section was located at the top (Top heat mode). The evaporator section was clamped to the heater block which the half-pipe wall contacted the heater block surface and the inner pipe wall being the fiber side. Heat input was supplied by a heater block at the upper end of the heat pipe, the bottom end of the heat pipe was also cooled by the circulation of air within a tunnel.

Actually, the heat pipe within smartphones do not have a fan to cool the condenser section. In the other hand, the experimental of this study aimed to compare the thermal performance of heat pipes. These were tested under same operating conditions thus the operating temperature (adiabatic temperature, T<sub>a</sub>) of the heat pipe was controlled as a constant value by using a fan for cooling system at condenser section. Therefore, the experimental setup was designed to work as closely as possible with the operation of heat pipes within smartphones. The cooling air in a tunnel was set as a laminar flow in order to slowly transfer the heat from the heat pipe.

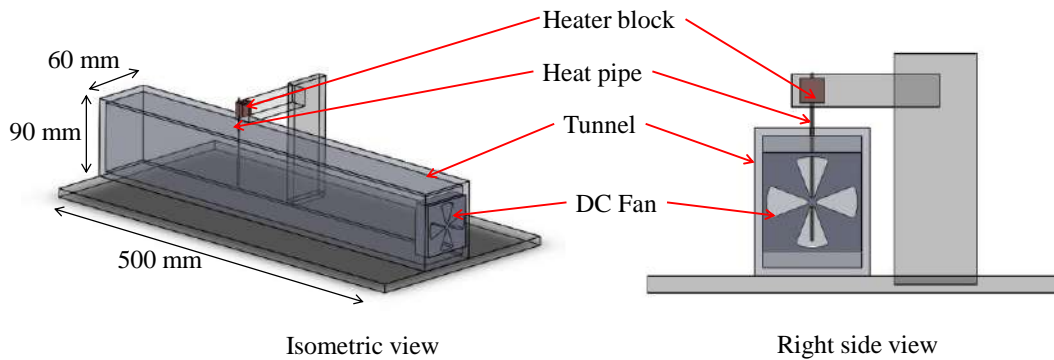


**Fig. 6.** The heat pipe thermal performance test rig.

The position to measure the temperature of evaporator, adiabatic and 2 points of condenser were 8, 18, 31 and 51 mm respectively as shown in Fig. 7. The temperatures were collected by K-type Chromel-Alumel thermocouples (Omega, accuracy  $\pm 0.5^\circ\text{C}$ ) which were displayed by temperature recorder brand LUTRON model BTM-4208SD offering temperature measurement accuracy with a marginal error of  $\pm 0.4^\circ\text{C}$ .

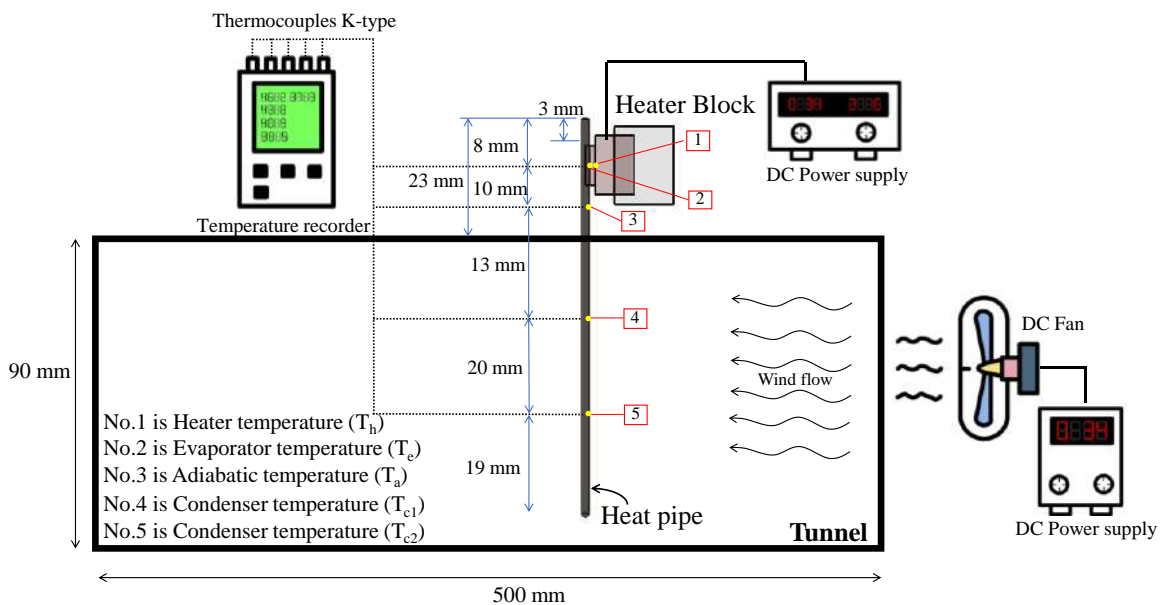


**Fig. 7.** The schematic diagram of experimental setup.

### 2.3 Experimental Procedure

During an experimental, the ambient temperature was controlled at  $25^\circ\text{C}$ . The experimental procedure consisted of 4 steps. First, the thermocouples were affixed to the heat pipe's outer surface at specified positions as depicted in Fig. 7. Second, the heat pipe was vertically clamped onto the heater block. Third, 1 W of heat input was supplied to the heater by adjustment both voltage and current of DC power supply while the adiabatic temperature was controlled at  $60^\circ\text{C}$  by fan speed adjustment. In this step, the maximum wind velocity which was applied to cool the heat pipe in the tunnel was 2.8 m/s. Finally, the temperatures were recorded when the temperature at all points were constant.

The process was iterated by incrementing the heat input at the evaporator by 1 W up to 4 W. For the ensuing steps, the repeating for 3 times of the procedures for each sample, aimed to investigate the influence of the fiber bundle wick configuration on heat pipe thermal performance.

After obtaining the experiment's temperature distribution results, the physical factors influencing the thermal characteristics of heat pipes were investigated. To determine the thermal resistance of heat pipe, the temperature distribution at various points along its length was used. The thermal resistance ( $Z$ , °C/W) which was used as a measure of the heat pipe performance could be obtained from Eqs. (2).

The experimental error was considered by calculating the propagation of error using Eqs. 2. The temperature error amounted to 0.4°C and the heat input ( $Q$ ) error was not constant, given that the heat input was recorded from the DC power supply with a voltage and current error of 0.1%. The heat input error fluctuated with the application of voltage and current to the heater. As a result, the average experimental error was 7.5%.

$$Z = \frac{T_e - T_c}{Q} \quad (2)$$

Where  $T_c = \frac{T_{c1} + T_{c2}}{2}$   
 $T_e$  was the evaporator temperature (°C).  
 $Q$  was the heat input (W).

### 3. Results and Discussion

#### 3.1 The Wall Temperature Distribution of Fiber Bundle Wick Heat Pipe

The wall temperature distribution of fiber bundle wick heat pipe in each configuration showed the same trend. Therefore, in this topic, the wall temperature distribution of fiber bundle wick heat pipe with mixing ratio 50%:50% pitch 10 mm was the only one configuration that was selected to show as in Fig. 8. The x-axis represented the length of heat pipe where the evaporator section at the top of the heat pipe started at 3 mm, the adiabatic section started at 13 mm and the condenser section started at 23 mm. The temperature distribution showed the temperature variation along the length of the pipe which indicated the thermal performance of the heat pipe. Low temperature differential between the evaporator section and condenser section indicated that the heat pipe could be effectively transferred the heat from the evaporator to the condenser sections. For the experimental results in this research, it was observed that temperature at the condenser section decreased with the increasing of distance from evaporator section. These could be clearly observed when the heat input increased, the temperature difference between the two condenser points were greater and the 2nd point ( $T_{c2}$ ) was lower temperature. It was shown that the heat transfer performance of the heat pipe decreased with increasing of heat input. This could be observed the increasing of the temperature difference between the evaporator section and the condenser section. Due to the return working fluid was resisted by gravity force it led to the evaporator section's lack of working fluid.

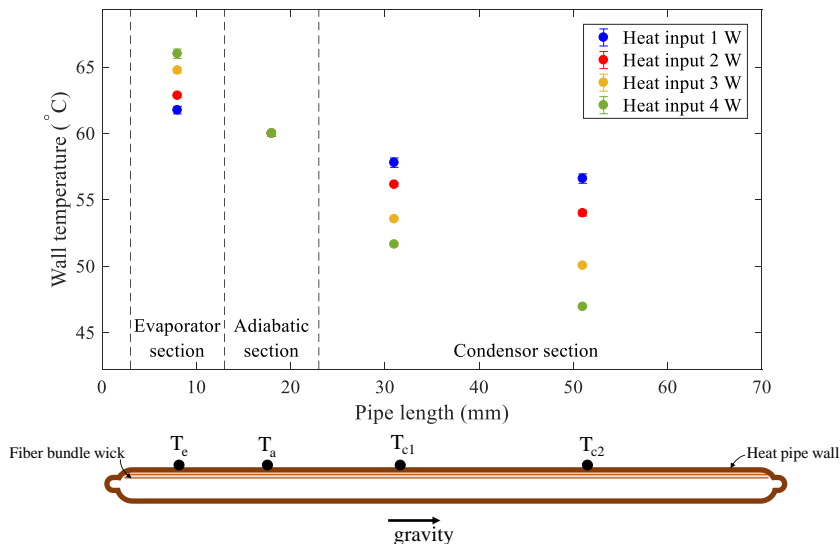


**Fig. 8.** The wall temperature distribution of fiber bundle wick heat pipe with mixing ratio 50%:50% pitch 10 mm.

### 3.2 Effects of Mixing Ratio on Thermal Resistance of Fiber Bundle Wick Heat Pipe

The effects of mixing ratio on thermal resistance in each configuration showed a similar trend. Due to the operation of the heat pipe with high heat input had low thermal performance. Therefore, the appropriate configurations focused on the maximum heat input as 4 W. The effects of mixing ratio on thermal resistance at heat input 4 W was shown as in Fig. 9. The x-axis represented the mixing ratio in percentage of fiber's diameter 30  $\mu\text{m}$  and 50  $\mu\text{m}$ . It was observed that for twist pitches of 10 mm and 15 mm, the thermal resistance decreased with the increasing of fiber's diameter 30  $\mu\text{m}$  until at 50% of fiber's diameter 30  $\mu\text{m}$  the thermal resistance increasing. So, the mixing ratio of 50%:50% demonstrated the lowest thermal resistance. Due to the appropriate pore size of the formed wick, it resulted in optimal capillary pressure and permeability.

However, the mixing ratio of 50%:50% at 20 mm pitch did not had the lowest thermal resistance. Because the larger pore size and loose twist with pitch 20 mm was unable to maintain small pore that resulted in the lower capillary pressure. Because the mixing ratio at 50%:50% had the equaling number of small (30  $\mu\text{m}$ ) and large (50  $\mu\text{m}$ ) fibers, resulted in the bundle had large pores more than others mixing ratio.

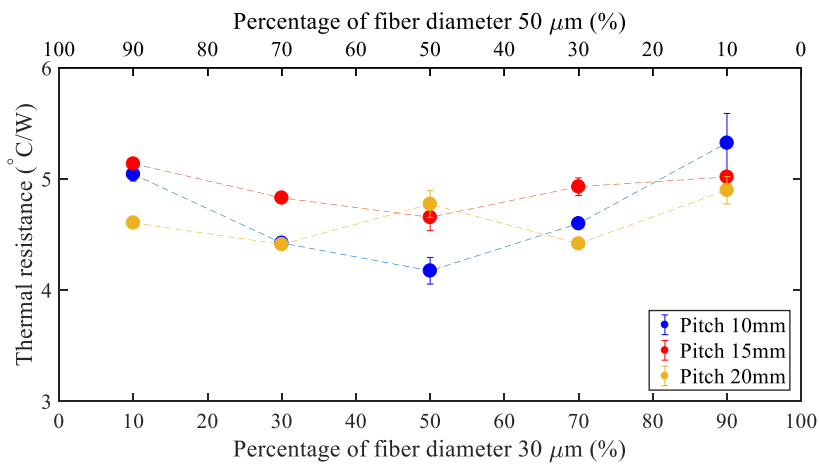


**Fig. 9.** Effects of mixing ratio on thermal resistance at heat input 4 W.

### 3.3 Effects of Pitch Length on Thermal Resistance of Fiber Bundle Wick Heat Pipe

The effects of pitch length on thermal resistance at heat input 4 W was shown in Fig. 10. The x-axis represented the pitch length in mm. Twisting with a high pitch mean twisting the fibers loosely as compared to twisting with a low pitch which means twisting the fibers more tightly. The liquid flowing through in the fiber bundle with low pitch (tight twist) had more tortuous, resulting in a lower permeability than a large pitch (loose twist). However, twisting with too much pitch (very loose twist) resulted in too large pore leading to low capillary pressure.

It was found that, the mixing ratio of 10%:90%, 30%:70% and 70%:30% were presented the same trend of thermal resistance. The 15 mm pitch length was maximum thermal resistance while the 20 mm pitch length was minimum thermal resistance. As the pitch length increased from 10 mm to 15 mm affecting to the thermal resistance increasing. The mixing ratio that had a greater number of large fibers (50  $\mu\text{m}$ ), was many large pores inside leading to low capillary pressure. Although the increasing of pitch (looser twist) provided a less tortuous flow channel, it was not sufficient. On other hand, the mixing ratio at 90%:10%, the thermal resistance were decreased. Because the greater number of small fibers (30  $\mu\text{m}$ ) than the large fibers (50  $\mu\text{m}$ ), the pore size was very small leading to higher capillary pressure combined with a looser twist makes the fluid flow less tortuous.

In additional, the pitch length increased from 15 mm to 20 mm with the thermal resistance decreasing. Because the tortuosity of the liquid flow was greatly reduced, the permeability to be greatly increased while maintaining a small pore size that could provided sufficient capillary pressure. On other hand, the mixing ratio at 50%:50%, the thermal resistance increased. Because of the equaling number of small fibers (30  $\mu\text{m}$ ) and large fibers (50  $\mu\text{m}$ ) resulted in the bundle had large pores more than others mixing ratio

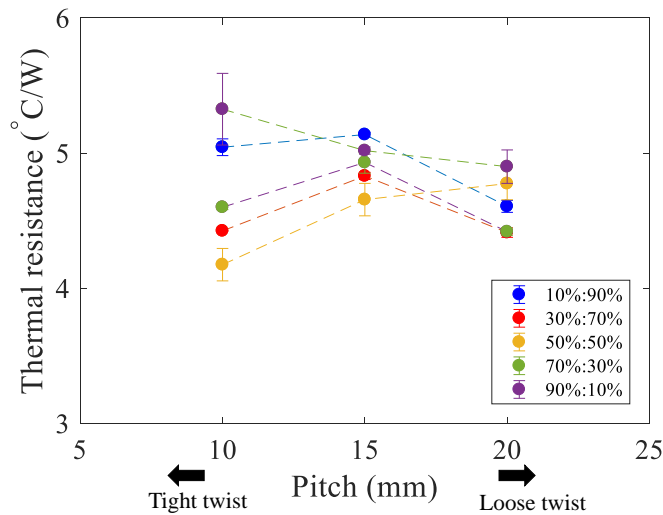


**Fig. 10.** Effects of pitch length on thermal resistance at heat input 4W.

### 3.4 The Optimal Configuration of Fiber Bundle Wick

Due to the operation of the heat pipe with high heat input had low thermal performance. Therefore, the appropriate configurations focused on the maximum heat input as 4 W. The optimal configuration of fiber bundle wick, providing the lowest thermal resistance, was the mixing ratio of 50%:50% with a pitch length of 10 mm as shown in Figs. 9 and 10. Because the appropriate pore size, the pores were formed from the equal number of small fiber (30  $\mu\text{m}$ ) and large fibers (50  $\mu\text{m}$ ), resulting in bigger pores than others mixing ratio. That means it had a high permeability. while twisting the with the tightest pitch (10 mm) made the individual fiber very tightly packed together, maintain the pore size as very small.

## 4. Conclusion

This research focused on the thermal performance of the heat pipe, with the new configuration of fiber bundle wick that were mixing of 30  $\mu\text{m}$  and 50  $\mu\text{m}$  fibers and twisted with 10, 15 and 20 mm pitch length, by using the experimental. The thermal resistance of the heat pipe was indicated the thermal performance. It was found that, the temperature at the condenser section decreased with the increasing of distance from evaporator section. Due to the return working fluid was resisted by gravity force, it led to the evaporator section's lack of working fluid.

Mixing ratio with a much higher number of fibers of a particular size, such as 10%:90% or 90%:10%, should be twisted with a pitch of 20 mm (loose twist) because the internal pore size was already very small. Twisting with a small pitch or tight twist reduced the permeability due to the more tortuosity of the flow channel. On the other hand, fiber bundle that had equal number of small fibers (30  $\mu\text{m}$ ) and large fibers (50  $\mu\text{m}$ ) which should be twisted with a pitch of 10 mm (tight twist) because the pores were already large leading to high permeability. Additionally, the tight twist helped maintain the pore size and also increasing capillary pressure due to the smaller pore size.

In this research, it was found that the optimal configuration of fiber bundle wick, providing the lowest thermal resistance, was the mixing ratio of 50%:50% with a pitch length of 10 mm.

## Acknowledgments

The presented work was financially supported by The Thailand Research Fund (TRF) and Fujikura Electronics (Thailand) Ltd. (Contract no. PHD58I0062). Furthermore, this research was conducted in Heat Pipe and Heat System Laboratory, Department of Mechanical Engineering, Faculty of Engineering, Chiang Mai University, Thailand.

## Nomenclature

CPUs	Central Processing Units
DC	Direct Current
d	Fiber's diameter, mm
FBW	Fiber bundle wick
g	Gravity, $m/s^2$
GPUs	Graphics Processing Units
K	Permeability, $m^2$
L	Length of bundle, mm
N	Number of fiber
%N	Percentage of number of fibers in bundle
P	Pitch length, mm
$P_c$	Capillary pressure, Pa
Q	Heat input, W
R	Radius, mm
T	Temperature, $^{\circ}C$
V	Volume, $mm^3$
Z	Thermal resistance, $^{\circ}C/W$
2D	Two-Dimensional

## Subscripts

a	Adiabatic section
c	Condenser section
c1	1 <sup>st</sup> position of the temperature measuring point at the condenser section
c2	2 <sup>nd</sup> position of the temperature measuring point at the condenser section
e	Evaporator section
h	Heater
w	Wick
1	Fiber's diameter 30 $\mu m$
2	Fiber's diameter 50 $\mu m$

## References

- [1] Hota SK, Lee KL, Leitherer B, Elias G, Hoeschele G, Rokkam S. Pulsating heat pipe and embedded heat pipe heat spreaders for modular electronics cooling. *Case Stud Therm Eng.* 2023;49:1-14.
- [2] Dobre T, Parvulescu OC, Stoica A, Iavorschi G. Characterization of cooling systems based on heat pipe principle to control operation temperature of high-tech electronic components. *Appl Therm Eng.* 2010;30(16):2435-2441.
- [3] Reay DA, Kew AP, McGlen RJ. *Heat pipe.* 6<sup>th</sup> ed. Oxford: Elsevier; 2014.
- [4] Kawahara Y, Mochizuki M, Saito Y, Horiuchi Y, Ahamed M. One-millimeter heat pipe and application to cooling module for electronic devices. *Fujikura Tech Rev.* 2011;40:34-38.
- [5] Lin YJ, Hwang KS. Effect of particle size and particle size distribution on heat dissipation of heat pipes with sintered porous wicks. *Metall Mater Trans A.* 2009;40(9):2071-2078.
- [6] Mochizuki M, Saito Y, Nguyen T, Mashiko K, Kumthonkittkun V, Kuriyama H, et al. The development of composite wick heat pipe. 1<sup>st</sup> International seminar on heat pipe and heat recovery system; 2004 Dec 8-9; Kuala Lumpur, Malaysia. p. 158-163.
- [7] Sauciuc I, Mochizuki M, Mashiko K, Saito Y, Nguyen T. The design and testing of the super fiber heat pipes for electronics cooling applications. Sixteenth Annual IEEE Semiconductor Thermal Measurement and Management Symposium; 2000 Mar 23; San Jose, USA. USA: IEEE; 2000. p. 27-32.
- [8] De Schampheleire S, De Kerpel K, Deruyter T, De Jaeger P, De Paepe M. Experimental study of small diameter fibres as wick material for capillary-driven heat pipes. *Appl Therm Eng.* 2015;78:258-267.
- [9] Grason GM. Geometry and optimal packing of twisted columns and filaments. *Rev Mod Phys.* 2015;87(2):401-419.

- [10] Loh CK, Harris E, Chou DJ. Comparative study of heat pipes performances in different orientations. Semiconductor Thermal Measurement and Management IEEE Twenty First Annual IEEE Symposium; 2005 Mar 15-17; San Jose, USA. USA: IEEE; 2005. p. 191-195.
- [11] Xiang J, Chen XB, Huang J, Zhang C, Zhou C, Zheng H. Thermal performances of anti-gravity heat pipe with tapering phase-change chamber. *Energies*, 2020;13(19):1-10.
- [12] Mueller GE. Numerical packing spheres in cylindrical. *Powder Technol.* 2005;159(2):105-110.
- [13] Mueller GE. Numerical simulation of packed beds with monosized spheres in cylindrical containers. *Powder Technol.*1997;92(2):179-183.
- [14] Thuchayapong N. Void fraction simulation of sintered wicks used in heat pipe [thesis]. Chiang Mai: Chiang Mai University; 2008.